American Journal of Pathology, Vol. 156, No. 1, January 2000


# Hepatocyte Cytokeratins Are Hyperphosphorylated at Multiple Sites in Human Alcoholic Hepatitis and in a Mallory Body Mouse Model

Conny Stumptner*, M. Bishr Omary,‡
Peter Fickert,† Helmut Denk,* and Kurt Zatloukal*

*From the Departments of Pathology* and Medicine,† University of Graz, Graz, Austria; and the Department of Medicine,‡ Palo Alto VA Medical Center and Stanford University, Palo Alto, California*

**Alcoholic hepatitis (AH) is associated with cytokeratin 8 and 18 (CK8/18) accumulation as cytoplasmic inclusion bodies, termed Mallory bodies (MBs). Studies with MB mouse models and cultured hepatocytes suggested that CK8/18 hyperphosphorylation might be involved in MB formation. However, no data exist on phosphorylation of CK8/18 in human AH. In this study, antibodies that selectively recognize phosphorylated epitopes of CK8 or CK18 were used to analyze CK8/18 phosphorylation states in normal human and murine livers, human AH biopsies, and livers of 3,5-diethoxycarbonyl-1,4-dihydrocollidine (DDC)-intoxicated mice, the last serving as model for MB induction. Hepatocyte cytokeratins become hyperphosphorylated at multiple sites in AH and in DDC-intoxicated mice. Hyperphosphorylation of CK8/18 occurred rapidly, after 1 day of DDC intoxication and preceded architectural changes of the cytoskeleton. In long-term DDC-intoxicated mice as well as in human AH, MBs preferentially contain hyperphosphorylated CK8/18 as compared with the cytoplasmic cytokeratin intermediate filament network suggesting that CK8/18 hyperphosphorylation may play a contributing role in MB pathogenesis. Furthermore, the site-specific phosphorylation of cytokeratin in different stages of MB induction provides indirect evidence for the involvement of a variety of protein kinases known to be activated in stress responses, mitosis, and apoptosis. *(Am J Pathol 2000, 156:77–90)***

Cytokeratins are members of the large family of intermediate filament (IF) cytoskeletal proteins, which are normally expressed in a tissue-specific manner and assembled as cytoplasmic filamentous arrays. Neurofilaments, α-internexin, desmin, vimentin, glial filaments, and the nuclear lamins[1,2] also belong to the IF family. The diverse cell biological functions of IFs are still poorly understood. However, a diversity of human diseases is associated with severe alterations of IFs. A common pathological feature of many IF-related diseases is the accumulation of intracytoplasmic inclusions consisting of modified IF proteins, for example in neurodegenerative diseases such as amyotrophic lateral sclerosis, Parkinson's disease, and Lewy body dementia[3–6]; in neuromuscular disorders (eg, spheroid body myositis[7]); and the formation of Mallory bodies (MBs) in alcoholic hepatitis (AH) and other liver disorders (eg, non-alcoholic steatohepatitis, Wilson's disease, primary biliary cirrhosis, Indian childhood cirrhosis, hepatocellular neoplasms[8–11]). Although the underlying pathogenetic mechanisms are as yet unclear, posttranslational modifications of IF proteins, such as phosphorylation, limited proteolysis, and cross-linking, may play a major role. For example, the presence of hyperphosphorylated neurofilament epitopes in some neuronal inclusion bodies[12–15] and of abnormally phosphorylated desmin in muscle fibers[16] were reported. Furthermore, a possible association of cytokeratin hyperphosphorylation with the formation of MBs in hepatocytes, a hallmark of AH, was suggested by *in vitro* and animal studies performed by our own group and others.[17–20]

AH follows chronic alcohol abuse and occurs in 20 to 40% of heavy drinkers. Although reversible at the beginning, most cases of AH progress to irreversible cirrhosis. Besides the amount of alcohol ingested per day, a variety of other factors such as dietary habits, genetic factors influencing alcohol metabolism, viral infections, and additional toxins or drugs seem to determine the extent of liver damage. Classical morphological features of AH are liver cell ballooning and necrosis, inflammation, steatosis, and the formation of cytokeratin-containing MBs, which is associated with severe derangement (ie, diminution or even loss) of the hepatocyte cytokeratin IF network.[8–11,22–26] Diverse animal models have been generated to study in more detail and under defined conditions mechanisms involved in the pathogenesis of this alcoholic liver disease. Experimental long-term intoxication of mice with

Supported by the grants of the Austrian Science Foundation S7401-MOB (to K. Z.) and 7628-MED (to H. D.) and by a U.S. Veterans Affairs Merit and Career Development Award (to M. B. O.).

Accepted for publication September 4, 1999.

Address reprint requests to Kurt Zatloukal, M.D., Division of Experimental Cell Research and Oncology, Department of Pathology, University of Graz, Auenbruggerplatz 25, A-8036 Graz, Austria. E-mail: kurt.zatloukal@kfunigraz.ac.at.

3,5-diethoxycarbonyl-1,4-dihydrocollidine (DDC) or griseofulvin (GF) mimics the particular hepatocellular alterations associated with AH, ie, ballooning of hepatocytes, accumulation of MBs, and alterations of the cytokeratin IF network.[27–31] These animal models are valuable not only for investigating the effects of long-term (chronic) intoxication (ie, for 2 to 4 months) but also for assessing the time course of alterations finally leading to MB formation and cytokeratin filament derangement. In addition to elucidating mechanisms involved in the pathogenesis of AH, these DDC and GF animal models may provide insight into biology and pathology of cytokeratins.

Cytokeratins are a multigene family consisting of at least 21 catalogued proteins.[2,32] According to sequence homology and biochemical properties they can be divided into two subgroups, the type I and type II cytokeratins, which form obligatory noncovalent heteropolymers that spontaneously assemble into 10-nm filaments.[2,33] Epithelia express characteristic patterns of type I and type II heteropolymers depending on their tissue origin and state of differentiation. For example, glandular and secretory simple type epithelia express cytokeratin 8 (CK8) and CK18 as their major cytokeratin pair with variable amounts of CK7, CK19, and CK20. Normal adult hepatocytes express CK8/18, which are equivalent to Endo A (CK8) and Endo B (CK18), originally described as cytokeratins A and D, in mouse hepatocytes.[34–36]

Cytokeratins undergo several posttranslational modifications, such as phosphorylation, glycosylation, acetylation, and transglutaminase-induced cross-linking, that are likely to be involved in regulating their function.[37–41] In the case of CK8/18, phosphorylation has been extensively studied in cultured cells and *in vitro* experiments. Phosphorylation of cytokeratins and other IF proteins plays important roles in the cell,[41] including regulation of filament disassembly and reorganization, particularly during mitosis, solubility, interaction with other proteins, and determining localization within specific compartments of the cell. With regard to CK8/18, phosphorylation occurs exclusively on serine residues and is increased during mitosis, apoptosis, growth factor stimulation, and different forms of cell stress. Various kinases seem to be involved in the phosphorylation of specific sites on either CK8 or CK18.[39–50] Several phosphorylation sites at the amino- and carboxy-terminal regions (termed head and tails, respectively) of cytokeratin proteins have been identified, such as serine 23 (Ser23), Ser73, and Ser431 in CK8 as well as Ser52 and Ser33 in CK18. Most if not all phosphorylation sites are located within these head and tail domains. Accumulating evidence indicates that they are important for filament assembly and interaction with other proteins. Recently, monoclonal and polyclonal antibodies selectively recognizing the various phosphoepitopes on CK8 or CK18 have been generated.[46–50] These antibodies provide ideal tools for studying the phosphorylation states of the various sites and their dynamics and topographical distribution in tissues and/or cultured cells.

Although many studies suggest a role for CK8/18 hyperphosphorylation in the pathogenesis of AH based primarily on the MB mouse models, there is no report about altered CK8/18 phosphorylation patterns in human AH compared to human control livers. We therefore investigated frozen tissue sections of liver biopsies with AH and human control livers using antibodies to four different phospho-epitopes on CK8/18 and determined the presence and distribution of the various CK8/18 phosphoepitopes. In addition, DDC-fed mice at different stages of intoxication were also studied to examine the time course of hepatocyte cytokeratin alterations under standardized experimental conditions.

In this report, we show that human and murine MBs contain CK8/18 phosphorylated at multiple sites. Moreover, phosphorylation levels and intracellular distribution of phosphorylated CK8/18 are altered in hepatocytes of human AH as well as DDC-intoxicated livers in comparison with control livers. This is the first demonstration that phosphorylation of hepatocyte CK8/18 is associated with human AH.

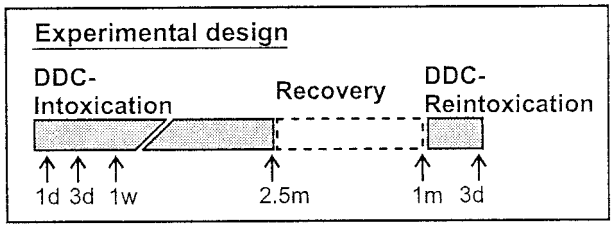


**Figure 1.** Schematic representation of the experimental design outlining the stages at which mice were used for various analyses described in Material and Methods. The recovery period is 1 month, which is followed by up to 3 days of reintoxication.

## *Materials and Methods*

### *Human Tissue Samples*

Human liver biopsy material was obtained from nine patients with histologically confirmed AH. Parts of the specimens were snap-frozen within 2 minutes after biopsy and stored in liquid nitrogen until analysis by immunofluorescence microscopy. Normal (control) liver parenchyma was obtained from the non-neoplastic margins of nine cases of surgically resected liver tumors.

### *Animal Model and Experimental Design*

Male Swiss Albino mice (35 g body weight; strain Him OF1 SPF; Institute of Laboratory Animal Research, University of Vienna School of Medicine, Himberg, Austria) were fed either a standard (control) diet (Altromin, Marek, Vienna, Austria) or a diet containing 0.1% DDC (Aldrich, Steinheim, Germany) for time periods ranging from 1 day to 2.5 months. After 2.5 months of continuous DDC feeding, some animals were allowed to recover on standard (control) diet for 1 month. Some of the recovered mice were then reintoxicated with DDC for 3 days. Figure 1 shows details of the experimental design. Mice were killed by cervical dislocation and the livers were snap-frozen in methylbutane precooled with liquid nitrogen for

**Table 1.** Primary Antibodies Used for Immunofluorescence Microscopy and Western Blotting

| Clone | Species | Antigen |
|---|---|---|
| 5B3 | M | CK8-pSer431 (h, m) |
| LJ4 | M | CK8-p-Ser73/79 (h/m) |
| Ks 8.7 | M | total CK8 pool (h, m) |
| Ks 18.04 | M | total CK18 pool (h, m) |
| 3055 | Rb | CK18-pSer52 (h) |
| 8250 | Rb | CK18-pSer33 (h, m) |
| 50K160 | Rb | total CK8+18 pool (h, m) |

M, mouse monoclonal antibody; Rb, rabbit polyclonal antibodies; h, human; m, murine.

immunohistochemistry and preparation of cytoskeletal proteins.

### *Immunofluorescence Microscopy*

Double-label immunofluorescence microscopy was performed on cryostat sections of liver tissue (3 μm thick, fixed in acetone at −20°C for 10 minutes) as described previously.[51] The antibodies directed against various epitopes (phosphorylated and nonphosphorylated) on CK8/18 are summarized in Table 1. The antibodies to phospho-CK8 (5B3, LJ4) or phospho-CK18 (8250, 3055) have been characterized recently.[46–50] The antibodies Ks 8.7, Ks 18.04 (Progen, Heidelberg, Germany), and 50K160[52] (also termed CK antibodies) were used to detect total CK8 and/or CK18 independent of phosphorylation state. As secondary antibodies, Cy2-conjugated goat anti-mouse IgG (Amersham, Buckinghamshire, UK) and tetramethylrhodamine isothiocyanate (TRITC)-conjugated swine anti-rabbit Ig (Dako, Glostrup, Denmark) were used. For control of background staining, the primary antibodies were omitted or replaced by IgG isotype control (Dako). Immunofluorescent stained specimens were analyzed with a MRC 600 (Bio-Rad, Richmond, CA) laser-scanning confocal device attached to a Zeiss Axiophot microscope. The fluorescent images were collected using the confocal photomultiplier tube at full frame (768 × 512 pixels). For dual labeling, separate excitation wavelengths (488 nm for Cy2, 568 nm for TRITC) from a krypton/argon ion laser were used.

### *Preparation of Cytoskeletal Proteins and Immunoblotting*

Cytoskeletal proteins were prepared from frozen mouse liver tissue by high salt-detergent extraction as described previously.[38] The following protease inhibitors were included in all buffers: 200 μmol/L pefabloc SC (Merck, Darmstadt, Germany), 50 mmol/L sodium fluoride (Merck), 0.3 μmol/L aprotinin (Boehringer Mannheim, Mannheim, Germany), 100 μmol/L leupeptin (Boehringer Mannheim), 1 μmol/L pepstatin (Boehringer Mannheim), 200 μmol/L sodium vanadate (Sigma, St. Louis, MO), and 1 mmol/L sodium pyrophosphate (Fluka, Buchs, Switzerland). Equal amounts of protein were electrophoresed on 10% sodium dodecyl sulfate-polyacrylamide gel electrophoresis[53] and electrophoretically transferred onto nitrocellulose membranes (0.2 μm pore size, Schleicher & Schuell, Dassel, Germany) with 0.1 A for 18 hours.[54] The membranes were blocked with 5% nonfat milk in TBS-T (10 mmol/L Tris-HCl, pH 7.4, 150 mmol/L NaCl containing 0.1% Tween-20) and incubated with the primary antibodies (5B3, 1:2000; LJ4, 1:1000; 8250, 1:2000 supplemented with 200 μg/ml nonphosphorylated peptide to prevent binding to the nonphosphorylated epitope) overnight at 4°C. After washing with TBS-T for 1 hour, the membranes were incubated with horseradish peroxidase-conjugated secondary antibodies (Dako) for 2 hours, followed by a final washing step in TBS-T for 1 hour. Antibody binding was detected using enhanced chemiluminescence (ECL, Amersham).

## *Results*

### *Hyperphosphorylation of CK8/18 in Human Alcoholic Hepatitis and Accumulation of Phosphorylated CK8/18 in Mallory Bodies*

In human control liver, CK antibodies that recognize cytokeratin independent of its phosphorylation state (Figure 2, a, c, e, and g) revealed a filamentous pattern with increased density at the cell periphery. Antibodies to phospho-CK8 (5B3) and phospho-CK18 (8250, 3055) preferentially stained this peripheral rim of cytokeratin filament bundles in the majority of hepatocytes (Figure 2). No staining with the phospho-CK8 antibody LJ4 (Figure 2, c and d) was obtained, suggesting that, in contrast to the other epitopes on CK8 and CK18, no phosphorylation of this site exists in human control liver.

In AH, CK antibodies (Figure 3, a, c, e, and g) revealed in some hepatocytes a derangement and diminution of the cytokeratin IF cytoskeleton and accumulation of CK8/18-containing MBs. All phospho-CK8 and phospho-CK18 antibodies intensely decorated MBs. However, LJ4 did react only with a subset of human MBs independent of their size (eg, Figure 3, c and d). In comparison with the staining pattern of phospho-CK8 antibodies in control liver, a shift in phospho-CK8 staining from the cell periphery to a pronounced staining of the cytoplasmic cytokeratin IF network occurred in AH (compare Figures 2 and 3). Moreover, immunostaining with LJ4, which was absent in control liver, became strongly positive in AH (Figure 3, c and d). The results obtained with antibodies to phospho-CK18 (8250, 3055; Figure 3, e-h) were similar but less conspicuous than that with phospho-CK8 antibodies (5B3, LJ4). The immunofluorescence results are summarized in Table 2.

### *Increase in CK8/18 Phosphorylation Is an Early Response to Hepatotoxicity Induced by DDC*

Prolonged feeding of mice with a DDC-containing diet has been widely used as an animal model for experimental induction of MBs with cytokeratin IF alterations similar to those associated with AH. We compared the phos-

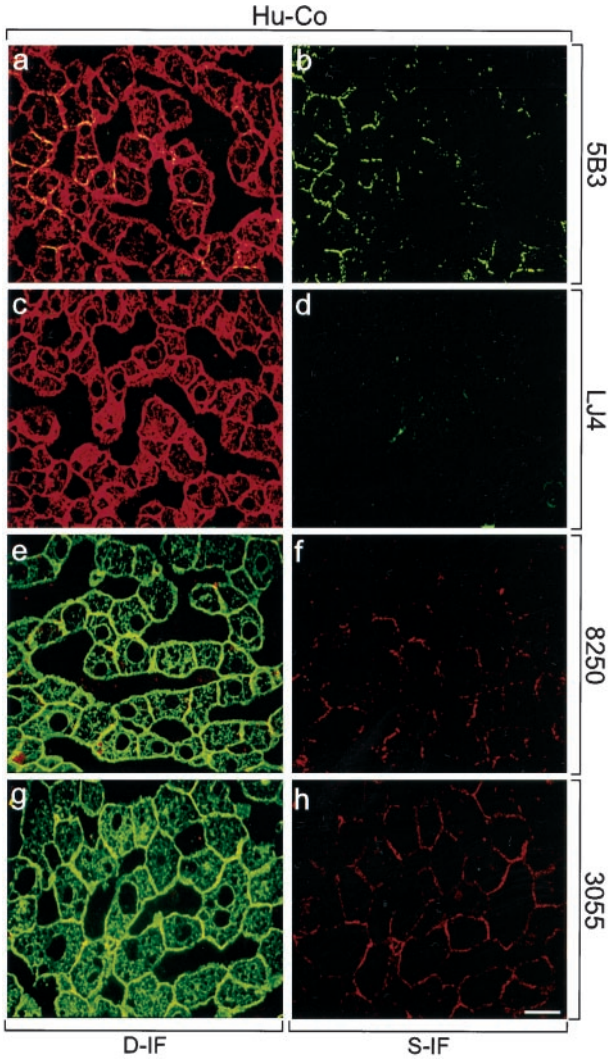


**Figure 2.** Distribution of phosphorylated CK8 or CK18, and total CK8/18 in human control liver (Hu-Co). Immunofluorescence double-labeling was performed on frozen tissue sections using antibodies to phospho-CK8 (5B3, LJ4; green in **a–d**), phospho-CK18 (8250, 3055; red in **e–h**), and to total CK8/18 (CK antibodies; red in **a, c;** green in **e, g**). Double- (D-IF) and corresponding single- (S-IF) label confocal micrographs are shown. 5B3, 8250, 3055: In Hu-Co liver, phospho-CK8/18 are preferentially located at the cell periphery. LJ4: There is no phosphorylation of the epitope recognized by LJ4 in Hu-Co liver. Bar = 20 $\mu$m.

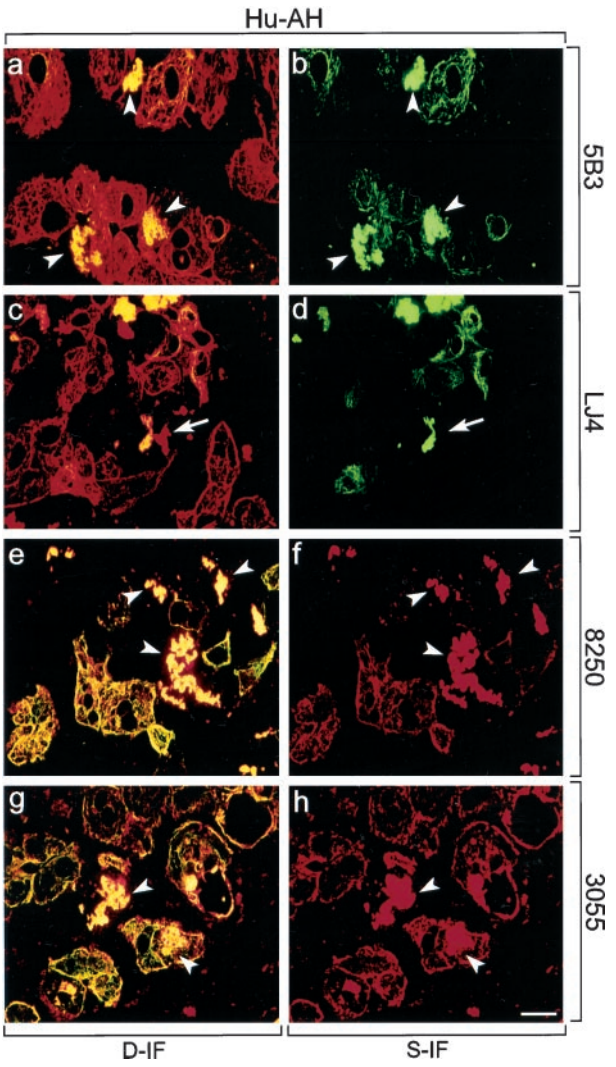


**Figure 3.** Distribution of phosphorylated CK8 or CK18, and total CK8/18 in human alcoholic hepatitis (Hu-AH). Immunofluorescence double-labeling was performed on frozen tissue sections using antibodies to phospho-CK8 (5B3, LJ4; green in **a–d**), phospho-CK18 (8250, 3055; red in **e–h**), and to total CK8/18 (CK antibodies; red in **a, c;** green in **e, g**). Double- (D-IF) and corresponding single- (S-IF) label confocal micrographs are shown. 5B3, 8250, 3055: Note the shift of phospho-CK8/18 staining in AH from the cell periphery to the whole cytoplasm with enhanced labeling of the cytokeratin filament network and of MBs. Examples of MBs are indicated by **arrowheads**. LJ4: In AH, immunoreactivity with cytokeratin filaments and with a subset of MBs is found. **Arrows** in **c** and **d** indicate nonreactive MBs. Bar = 20 $\mu$m.

phorylation patterns of CK8/18 in control mice, in mice at different stages of DDC intoxication (ie, short-term treatment for 1 to 7 days, and long-term treatment for 2.5 months), in mice that were allowed to recover for 1 month on control diet after 2.5 months of DDC feeding, and in mice reintoxicated with DDC for 3 days after an initial DDC intoxication and subsequent recovery period (see Materials and Methods and Figure 1). Immunofluorescence microscopy was performed on frozen liver sections with antibodies that were used in Figure 2, except for the 3055 antibody, which does not cross-react with mouse CK18.

In livers of mice fed a control diet, hepatocytes displayed a regular cytokeratin IF network stained with CK antibodies (Figure 4, a, c, and e), whereas phospho-CK8 antibodies 5B3 and LJ4 did not stain (Figure 4, b and d), except for a few single cells (<0.1%, not shown). Phospho-CK18 antibody 8250 preferentially decorated the cytokeratin filaments at the cell periphery (Figure 4, e and f). However, after only 1 day of DDC intoxication, a dramatic increase in phosphorylation, particularly of CK8, was obvious. The staining pattern of phospho-CK8 antibody 5B3 resembled that revealed by CK antibodies, ie, staining of the cytoplasmic cytokeratin network with accentuation of the cell periphery and around the bile canaliculi (Figure 5, a and b). In contrast the distribution of LJ4 reactivity was patchy, with clusters of 2 to 5 cells showing bright cytoskeletal staining and other cells displaying only slight reactivity at the cell periphery (Figure 5, c and d). Immunostaining with anti-phospho-CK18 (8250) was similar to

**Table 2.** Summary of Immunofluorescence Results Obtained with Antibodies to Phospho-CK8 (5B3, LJ4) and to Phospho-CK18 (8250) on Human Control Livers and Human Alcoholic Hepatitis

| | 5B3 | | | LJ4 | | | 8250 | | | 3055 | | |
|---|---|---|---|---|---|---|---|---|---|---|---|---|
| | P | CK | MB | P | CK | MB | P | CK | MB | P | CK | MB |
| Hu-Co | ++ | + | 0 | − | − | 0 | + | − | 0 | + | − | 0 |
| Hu-AH | + | ++ | +++ | + | + | +++ | + | + | +++ | + | + | +++ |

The degree of staining was estimated from − (no staining) to +++ according to the intensity and percentage of labeled cells. 0, no MBs present.
Hu-Co, control liver; Hu-AH, alcoholic hepatitis; P, cytokeratin staining at the cell periphery; CK, staining of the whole cytoplasmic cytokeratin IF network; MB, Mallory bodies.

5B3 but slightly weaker. Because CK18 was phosphorylated at a low basal level in control mouse liver, the increase in phosphorylation on DDC intoxication was not as conspicuous as that observed for CK8. The red aggregates in hepatocytes and sinusoidal spaces (eg, Figures 5–8, e and f) represent autofluorescent porphyrin deposits, which accumulate in the liver on DDC intoxication. These aggregates were also seen in the corresponding negative controls where the first antibodies had been omitted (not shown). After 2.5 months of DDC intoxication, mouse hepatocytes showed the characteristic derangement of the cytokeratin IF system as revealed by immunostaining with CK antibodies. The staining changes included loosening or loss of the (immunostainable) cytokeratin IF network and accumulation of MBs (Figure 6). As in AH, phospho-CK8/18 antibodies (5B3, LJ4, 8250) brightly decorated MBs and the cytokeratin IF network of numerous hepatocytes (Figure 6). Although phospho-cytokeratins were obviously integrated in the cytokeratin IF network, in some hepatocytes they preferentially accumulated in MBs. In these hepatocytes phospho-CK8 antibodies strongly reacted with MBs but did not stain the cytokeratin network adjacent to the MBs (eg, asterisk in Figure 6, c and d). With LJ4, however, occasional MBs independent of their size were negative or only weakly stained (not shown).

To examine the dynamics of CK8/18 phosphorylation we used long-term DDC-intoxicated and then recovered mice, a situation that leads to gradual restoration of the cytoskeletal architecture. Reintoxication of these primed mice with DDC results rapidly (within 3 days) in MB reappearance and cytokeratin IF disturbance identical to those observed after initial long-term (2.5 months) DDC intoxication. To correlate reversibility and rapid reappearance of these cytokeratin-associated alterations with possible changes in CK8/18 phosphorylation, we performed immunofluorescence microscopy on frozen liver sections of recovered and reintoxicated mice. The staining of livers of mice recovered from long-term DDC intoxication closely resembled control livers (Figure 7). Residual alterations were the presence of few hepatocytes without detectable cytokeratin network but with small MBs mostly at the cell periphery (arrowheads in Figure 7). Phosphorylation of CK8/18 returned to normal, ie, no staining of the cytokeratin filaments with phospho-CK8 antibodies (5B3, LJ4) and weak staining of the cytokeratins predominantly at the cell periphery with anti-phospho-CK18 (8250). However, 5B3 and 8250 staining was still present in MBs (Figure 7, a, b, e, and f), whereas LJ4 did not recognize residual MBs (Figure 7, c and d). On reintoxication, a profound increase in CK8/18 phosphorylation was observed within 3 days (Figure 8, a-f). Cytokeratin filaments were strongly stained by 5B3, LJ4, and 8250 antibodies. Newly formed MBs present at the intersections of the cytokeratin IF network were also brightly stained with 5B3 and 8250 (Figure 8). As already observed in mice fed DDC for 2.5 months, there was preferential staining of MBs with antibodies to phospho-CK8, whereas the residual cytokeratin IF network of the hepatocytes that contained the MBs remained unstained. The phospho-CK8 antibody LJ4 did not stain the majority of these small, apparently newly formed MBs. Hence, phosphorylation of CK8 at this particular site (ie, phospho-Ser73, which is recognized by LJ4) displays a different response to DDC in that it appears late in the process of MB formation, as seen in reintoxicated mice, but disappears early, as shown in recovered mice. A summary of the immunofluorescence results is shown in Table 3.

To further verify the profound changes in phosphorylation of hepatic CK8 in DDC-intoxicated mouse livers, Western blots with the antibodies to phospho-CK8 (5B3, LJ4) and to total CK8 (Ks 8.7) were performed. No reactivity with phospho-CK8 antibodies (5B3 and LJ4) was found in control liver cytokeratin preparations, although a band corresponding to CK8 was recognized by Ks 8.7 (Figure 9). A clear-cut increase in CK8 phosphorylation was detectable within 1 week of DDC intoxication and persisted for the whole DDC intoxication period (2.5 months). On withdrawal of DDC and recovery, CK8 phosphorylation level was reduced but rose again on DDC reintoxication. These immunoblotting results are in line with the immunofluorescence data in that dramatic and site-specific CK8 hyperphosphorylation in response to DDC intoxication was noted. Moreover, the immunostaining with phospho-CK8 antibodies of the cytokeratin IF network as seen in immunofluorescence microscopy as well as the presence of hyperphosphorylated CK8 in the cytoskeletal insoluble fraction as analyzed by Western blotting, suggested that phosphorylated CK8 was able to form IF structures *in vivo*.

## Discussion

The essential role of the cytokeratin IF cytoskeleton in disease has been highlighted by the discovery that cytokeratin mutations are the primary cause of diverse forms of blistering skin diseases.[2,55,56] Furthermore, genetic alteration of cytokeratins is a potential pathogenetic factor in diseases of organs other than the skin because, for instance, a mutation in CK18 has recently been iden-

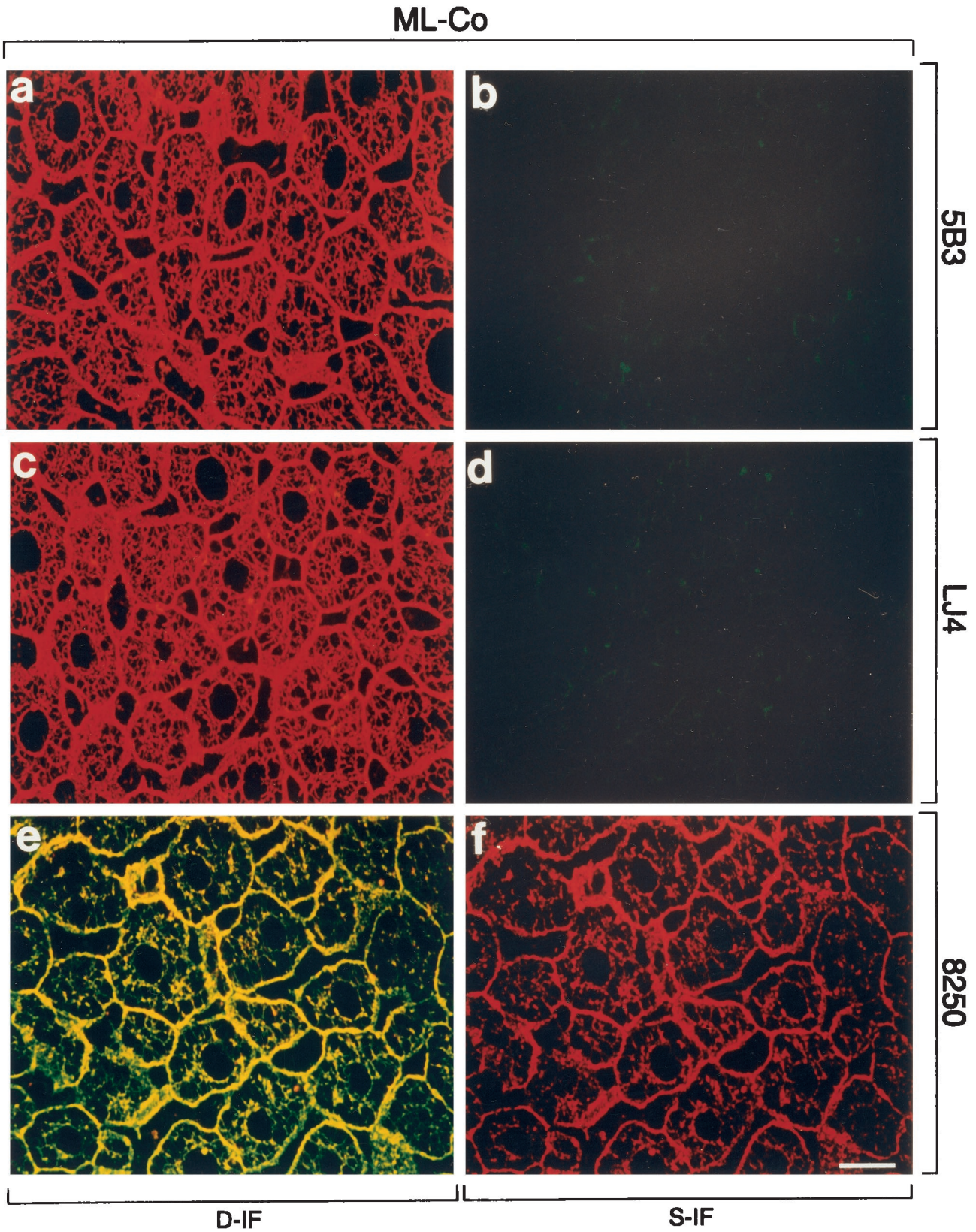


**Figure 4.** Distribution of phosphorylated CK8 or CK18 and total CK8/18 in normal livers of mice fed a control diet (ML-Co). Immunofluorescence double-labeling was performed on frozen tissue sections using antibodies to phospho-CK8 (5B3, LJ4; green in **a–d**), phospho-CK18 (8250; red in **e, f**), and to total CK8/18 (red in **a, c;** green in **e**). Double- (D-IF) and corresponding single- (S-IF) label confocal micrographs are shown. There is no immunoreactivity for 5B3 and LJ4, except weak sinusoidal background staining caused by the anti-mouse secondary antibody. 8250 stains the cytokeratin filament cytoskeleton at the cell periphery and throughout the cytoplasm. Bar = 20 $\mu$m.

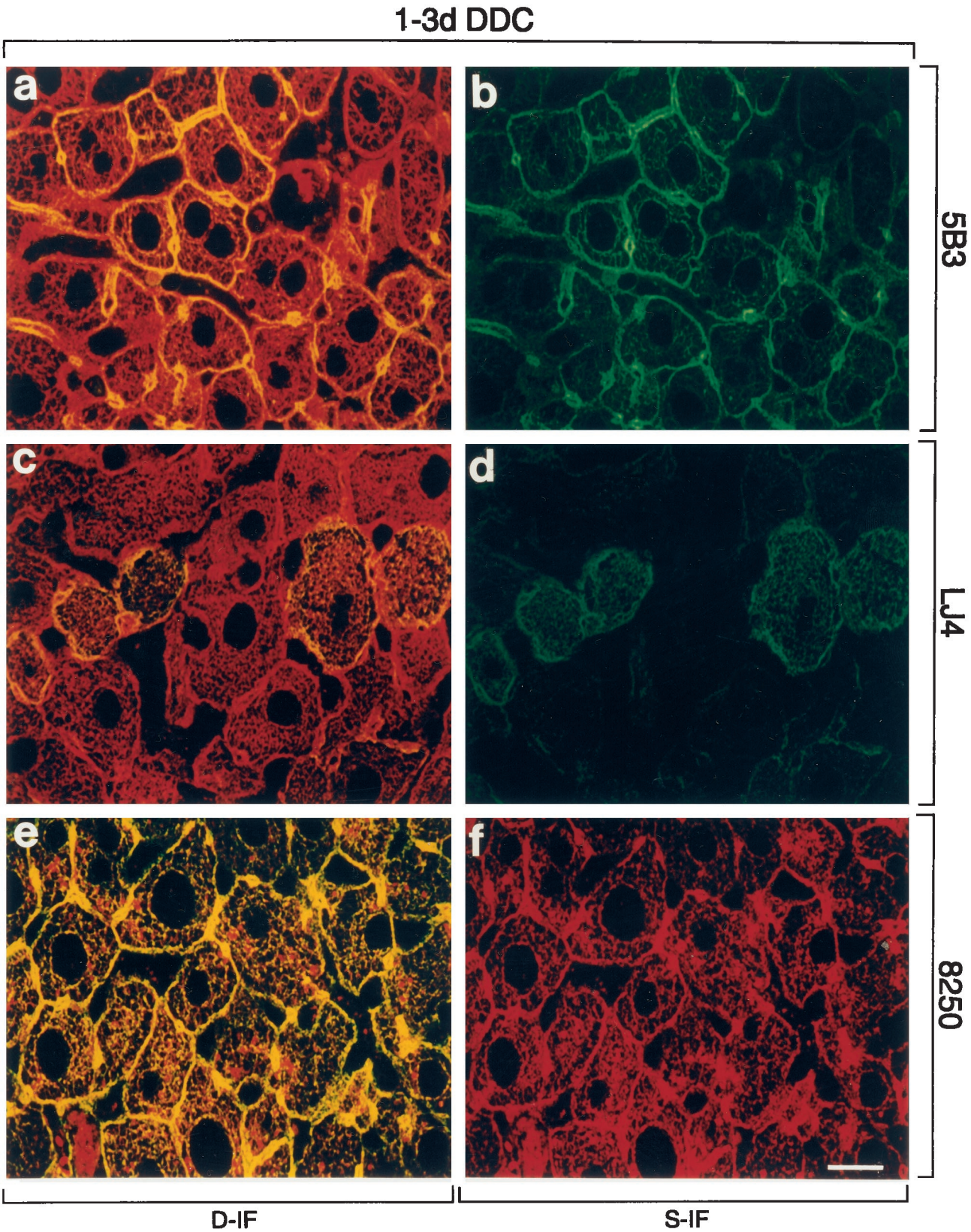


**Figure 5.** Distribution of phosphorylated CK8 or CK18 and total CK8/18 in intoxicated livers of mice fed a DDC-containing diet for 1 or 3 days (1 day in **a, b, e,** and **f** or 3 days in **c** and **d**). Immunofluorescence double-labeling was performed on frozen tissue sections using antibodies to phospho-CK8 (5B3, LJ4; green in **a–d**), phospho-CK18 (8250; red in **e, f**), and to total CK8/18 (red in **a, c;** green in **e**). Double- (D-IF) and corresponding single- (S-IF) label confocal micrographs are shown. 5B3, LJ4, 8250: In DDC-intoxicated mice, staining of the peripheral and cytoplasmic cytokeratin filaments is observed. Red aggregates in **e** and **f** represent autofluorescent porphyrin-containing pigment deposits, which accumulate on DDC intoxication. Such aggregates were also seen in corresponding negative controls. Bar = 20 $\mu$m.

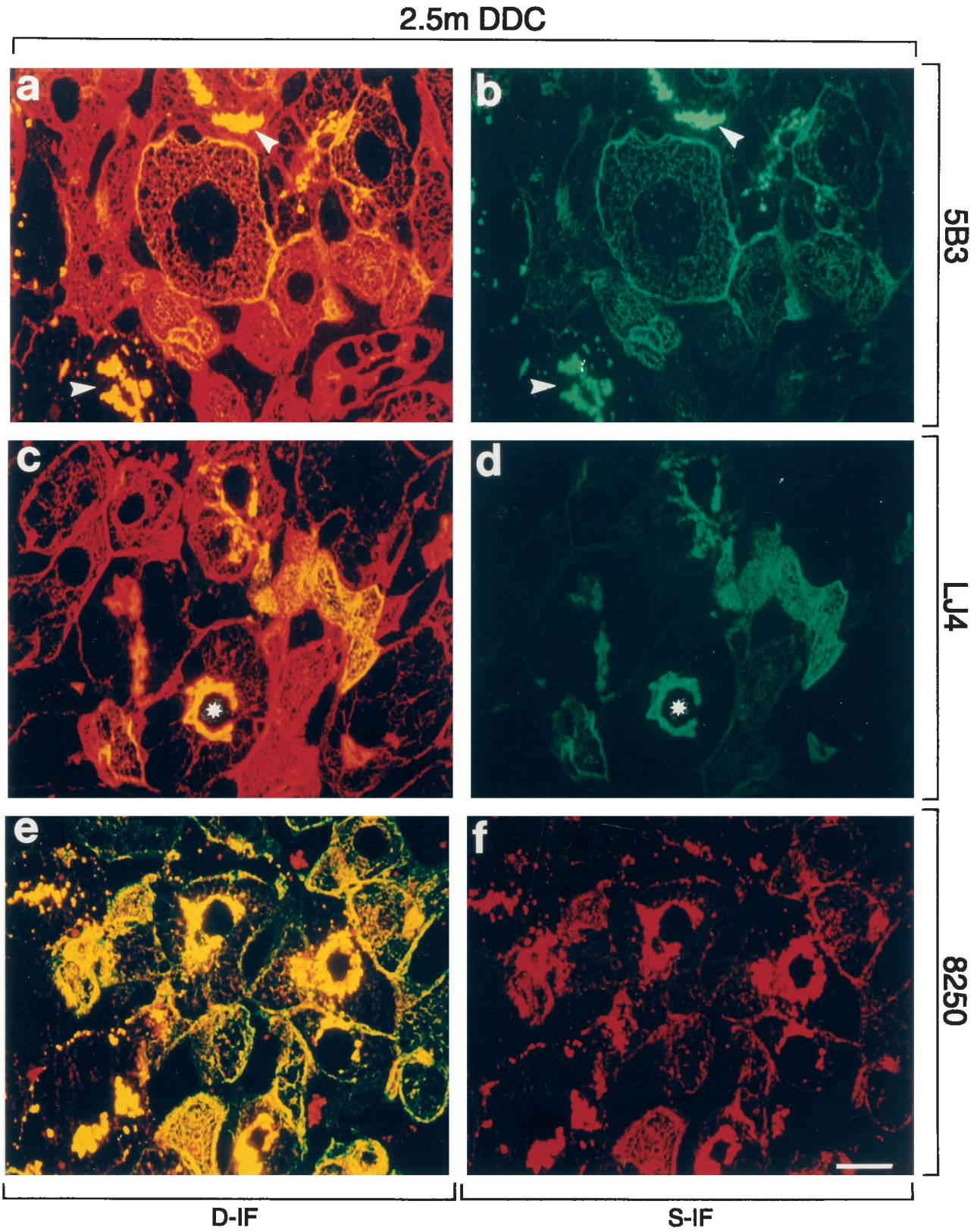


**Figure 6.** Distribution of phosphorylated CK8 or CK18 and total CK8/18 in intoxicated livers of mice fed a DDC-containing diet for 2.5 months (2.5 m DDC). Immunofluorescence double-labeling was performed on frozen tissue sections using antibodies to phospho-CK8 (5B3, LJ4; green in **a–d**), phospho-CK18 (8250; red in **e, f**), and to total CK8/18 (red in **a, c;** green in **e**). Double- (D-IF) and corresponding single- (S-IF) label confocal micrographs are shown. 5B3, LJ4, 8250: In many hepatocytes cytokeratin filaments and MBs (**arrowheads**) are brightly stained with antibodies to phospho-CK8/18. Note that in some hepatocytes only MBs are immunoreactive, whereas the cytokeratin IF network remains unstained (**asterisk** in **c** and **d**). Red aggregates in **e** and **f**, also present in negative controls, represent autofluorescent porphyrin deposits (see Figure 4). Bar = 20 $\mu$m.

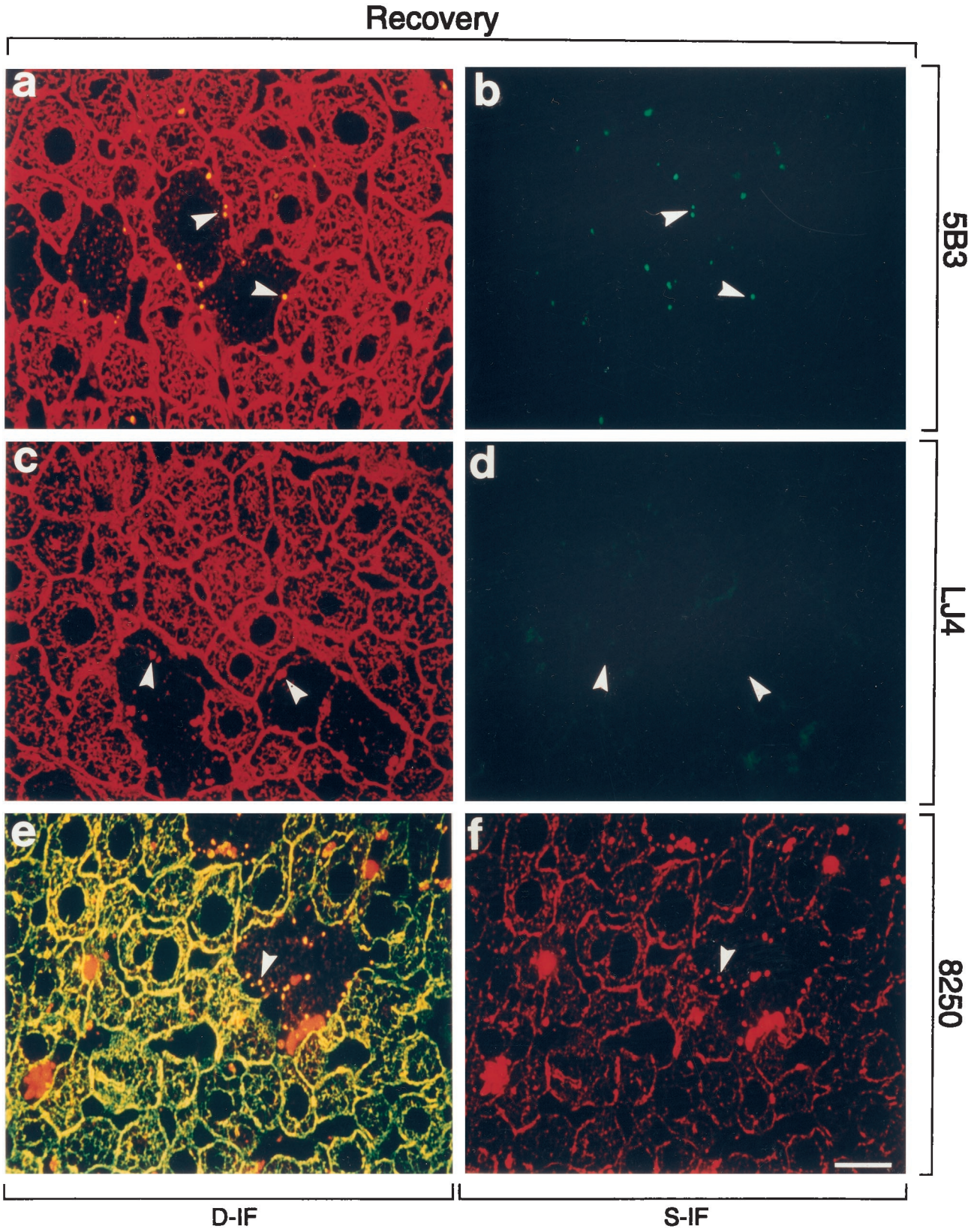


**Figure 7.** Distribution of phosphorylated CK8 or CK18 and total CK8/18 in livers of DDC-intoxicated (2.5 months) and recovered (1 month) mice (Recovery). Immunofluorescence double-labeling was performed on frozen tissue sections using antibodies to phospho-CK8 (5B3, LJ4; green in **a–d**), phospho-CK18 (8250; red in **e, f**), and to total CK8/18 (red in **a, c;** green in **e**). Double- (D-IF) and corresponding single- (S-IF) label confocal micrographs are shown. Only small MBs are detected by 5B3. There is no reaction of LJ4, except weak sinusoidal staining caused by the anti-mouse immunoglobulin secondary antibody. 8250 stains small MBs and cytokeratin IF bundles predominantly at the cell periphery. **Arrowheads** in **a–f** indicate examples of small (residual) MBs. Red aggregates in **e** and **f** represent autofluorescent porphyrin deposits (see Figure 4). Bar = 20 $\mu$m.

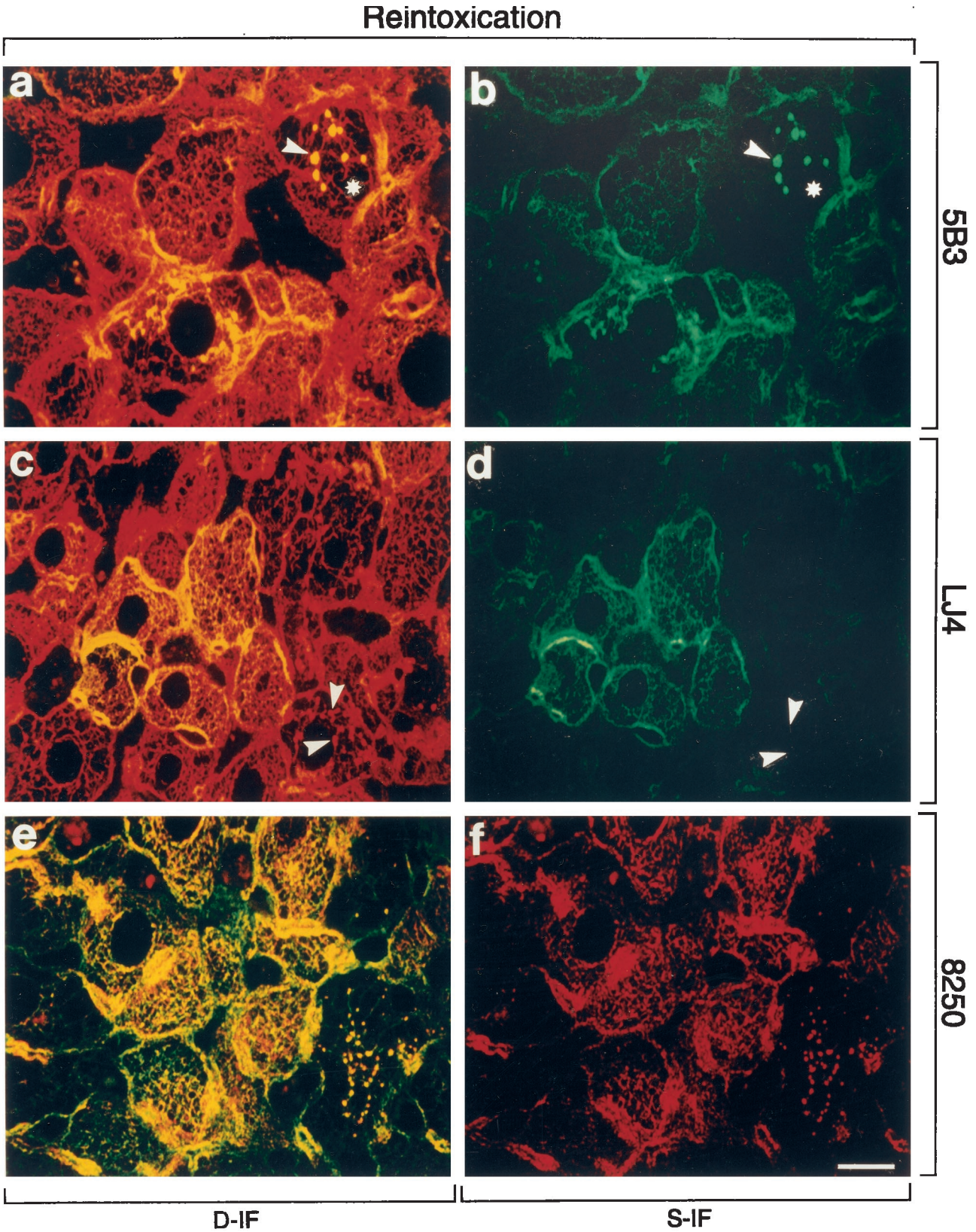


**Figure 8.** Distribution of phosphorylated CK8 or CK18 and total CK8/18 in livers of mice reintoxicated with DDC for 3 days after initial intoxication for 2.5 months and 1 month recovery (Reintoxication). Immunofluorescence double-labeling was performed on frozen tissue sections using antibodies to phospho-CK8 (5B3, LJ4; green in **a–d**), phospho-CK18 (8250; red in **e, f**), and to total CK8/18 (red in **a, c;** green in **e**). Double- (D-IF) and corresponding single- (S-IF) label confocal micrographs are shown. 5B3, 8250: In many hepatocytes, cytokeratin filaments and/or MBs are brightly stained with antibodies to phospho-CK 8/18. Examples of MBs are indicated by **arrowheads**. Note that in some hepatocytes only MBs are immunostained, whereas the cytokeratin-IF network remains unstained (**asterisk** in **a** and **b**). LJ4: The majority of MBs is not labeled by LJ4 (**arrowheads**). Red aggregates in **e** and **f** represent autofluorescent porphyrin deposits (see Figure 4). Bar = 20 $\mu$m.

**Table 3.** Summary of Immunofluorescence Results Obtained with Antibodies to Phospho-CK8 (5B3, LJ4) and to Phospho-CK18 (8250) on Livers of Control and DDC-Intoxicated Mice

| | 5B3 | | LJ4 | | 8250 | |
|---|---|---|---|---|---|---|
| | CK | MB | CK | MB | CK | MB |
| Co | − | 0 | − | 0 | +/− | 0 |
| 1 d DDC | + | 0 | + | 0 | +/− | 0 |
| 3 d DDC | ++ | 0 | +/++ | 0 | + | 0 |
| 1 w DDC | +++ | 0 | ++/+++ | 0 | ++/+++ | 0 |
| 2.5 m DDC | ++ | +++ | ++ | ++ | +/++ | +++ |
| Recovery | − | ++ | − | − | +/− | ++ |
| Reintox. | ++ | +++ | +/++ | + | +/++ | +++ |

CK, cytokeratin filaments; MB, Mallory bodies; Co, control diet; 1 d DDC, DDC-containing diet for 1 day; 3 d DDC, DDC-containing diet for 3 days; 1 w DDC, DDC-containing diet for 1 week; 2.5 m DDC, DDC-containing diet for 2.5 months; Recovery, 1 month control diet after 2.5 months of DDC feeding; Reintoxication, DDC feeding for 3 days after 1 month recovery.

The degree of staining was estimated from − (no staining) to +++ according to the intensity and percentage of labeled cells. 0, no MBs present.

tified in a case of cryptogenic liver cirrhosis.[57] Structure and function of the cytokeratin IF cytoskeleton is not only affected by gene mutations but is also rapidly and reversibly modulated by posttranslational modifications, thus making the cytokeratin IF cytoskeleton a potential target for a variety of environmental factors.[41] Phosphorylation is one of the most important means of regulating protein function in response to extracellular stimuli. It has recently been shown in mice that CK8 and CK18 become phosphorylated as a consequence of toxic liver injury induced by a variety of substances, such as GF and microcystin.[17,19,58,59] This hyperphosphorylation of cytokeratin appeared to be involved in the cellular response to toxic stress and is not a mere epiphenomenon due to a general deregulation of protein phosphorylation in the course of cell damage. The clearly demonstrated association of increased CK8/18 phosphorylation with a variety of cell stresses[41,60] has been substantiated recently as having a direct or indirect effect on protection from hepatotoxic injury. As such, transgenic mice that overexpress CK18 that is mutated at Ser52 are more susceptible to microcystin- and GF-induced liver injury as compared to mice that overexpress wild-type CK18.[59] The mechanism by which stress-induced cytokeratin hyperphosphorylation protects against certain types of liver injury remains an open question.

Using a panel of monoclonal antibodies that are specific for various phosphorylation sites on CK8 and CK18, we report here on marked phosphorylation of cytokeratins at multiple sites in human toxic liver injury, namely AH, and accumulation of phosphorylated cytokeratin material in MBs. The strong reactivity of MBs and, to a variable extent, of the cytokeratin IF cytoskeleton of hepatocytes with all phospho-cytokeratin-specific antibodies tested implies involvement of different protein kinases and/or phosphatases in this disease. The phosphorylation sites recognized by these antibodies have been characterized in previous studies, giving rise to speculation about the mechanisms leading to their phosphorylation and the biological consequences. For example, phosphorylation of CK8 at Ser73 as detected by LJ4 occurs preferentially in response to stress situations but is also seen during apoptosis and mitosis.[46] Although phosphorylation of IF proteins generally results in their disassembly and increased solubility, phosphorylation of Ser73 is significantly associated with the insoluble cytokeratin fraction.[46] Furthermore, phosphorylation-induced disassembly of cytokeratin proteins may indirectly support their aggregation with other MB components, because MBs form not from cytokeratin IF but from disassembled cytokeratin proteins (Zatloukal K, Stumptner C, Lehner M, Deuk H, Baribault H, Eshkind LG, Franke WW, manuscript submitted). In this context it is interesting that we observed in AH as well as in DDC-treated mice a subpopulation of hepatocytes where phosphorylated cytokeratin accumulated in MBs but was not detectable in the cytokeratin IF network adjacent to the MBs. Based on the observed immunoreactivities of MBs with the antibodies 5B3, 3055, and 8250, it is likely that a variety of protein kinases, such as ERK1/2, which phosphorylates CK8 at Ser431,[49] or PKC and cdc2 kinases, which can phosphorylate CK18 at Ser52[47] and Ser33,[50] respectively, are activated in AH and in DDC-fed mice (for summary of results, see Tables 2 and 3). This is in line with and extends previous reports on the effect of ethanol on the activation of several protein kinases, such as PKC, JNK, and p42/44 MAPK, that are involved in different signal transduction pathways.[61,62] Because of the complexity of alterations induced by ethanol and DDC intoxication, one must take into account that besides the cytokeratin IFs, a variety of other cellular proteins are affected as well and thus could contribute to the observed cytoskeletal changes.

To further dissect this complex situation and to get more insights into the course of cytokeratin phosphorylation during intoxication, we analyzed mice after different periods of DDC feeding, recovery from intoxication, and re-exposure to DDC. Phosphorylation of cytokeratin was already detectable at 1 day after commencement of DDC feeding; thus it is one of the earliest changes seen after intoxication that precedes structural alterations of the cytokeratin IF network. In contrast to the phosphorylation of Ser33 on CK18 (as detected by 8250) and Ser431 on CK8 (as detected by 5B3), which was seen in the majority of hepatocytes and, therefore, could reflect a cellular response to the metabolism of DDC, phosphorylation of Ser73 on CK8 (as detected by LJ4) was found in only a few cells. The distribution pattern of LJ4-reactive hepatocytes, typically as cell doublets, suggests that some of these cells represent daughter cells generated by mito-

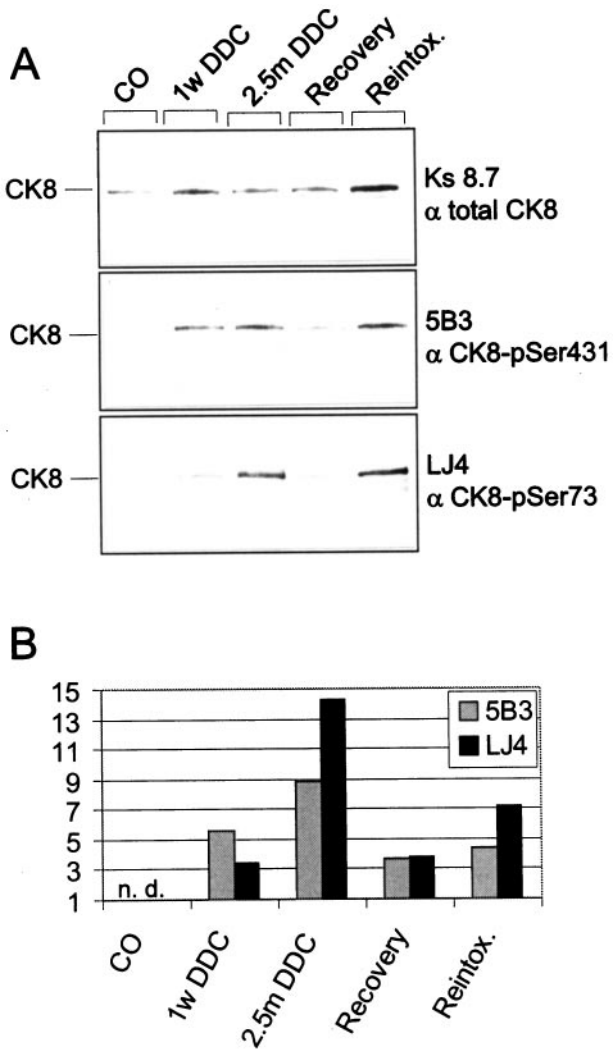


**Figure 9.** Phosphorylation of CK8 in DDC-intoxicated mouse livers. Cytoskeletal fractions were prepared from livers of control and DDC-intoxicated mice. Equal amounts of protein were separated by sodium dodecyl sulfate-polyacrylamide gel electrophoresis, electroblotted onto nitrocellulose membranes, and then stained with antibodies to phospho-CK8 (5B3, LJ4) and to the total CK8 pool (Ks 8.7). The Western blot is shown in **A** and the densitometric analyses of the band intensities using a Docu Gel V video densitometer (MWG Biotech, Ebersberg, Germany) and Rflp-scan software (MWG Biotech) are shown in **B**. The bars indicate the relative amount of phosphorylated CK8 as detected by 5B3 and LJ4 normalized to total CK8 as revealed by Ks.8.7. Abbreviations: n.d., not detectable; CO, control diet; 1 w DDC, DDC-containing diet for 1 week; 2.5 m DDC, DDC-containing diet for 2.5 months; Recovery, 1 month control diet after 2.5 months of DDC-feeding; Reintox., DDC-feeding for 3 days after 1 month recovery.

sis. This is also supported by the previous observations that the LJ4 epitope is generated during mitosis in addition to stress situations. In mice intoxicated long-term, the difference in the staining patterns of the antibodies 8250, 5B3, and LJ4 was less clearly revealed. Here, scattered groups of hepatocytes showed phosphorylation of the cytokeratin network to a variable extent. Furthermore, MBs were stained, as in human AH, by all three antibodies. There were, however, some MBs that did not stain with LJ4. Differences in the phosphorylation pattern of MBs were more clearly revealed in reintoxicated mice where newly formed MBs could be studied.[63] In these mice 8250 and 5B3 strongly reacted with small MB granules at the intersections of the cytokeratin IF network, representing the earliest detectable phase of MB formation. The phosphorylation of the epitopes recognized by these two antibodies may, therefore, participate in the initiation of MB formation. In contrast to 8250 and 5B3, LJ4 did not react with newly formed MBs, which shows that phosphorylation of Ser73 on CK8 (the epitope recognized by LJ4) is not involved in early MB formation. In more advanced stages of MB formation, however, phosphorylation of the LJ4 epitope could contribute to the growth of MBs, since we observed in later phases of reinduction as well as in the mice intoxicated with DDC for 2.5 months a subpopulation of hepatocytes with large MBs where LJ4 reacted with the MB but did not stain the residual cytokeratin network adjacent to the MB.

Further differences in the immunoreactivity profile of MBs at different phases of development were seen in mice at 1 month after recovery from intoxication. In contrast to 8250 and 5B3, which decorated small MB remnants at the cell periphery, LJ4 did not bind to MBs in these livers. This indicates that some protein kinases were still active even 1 month after cessation of intoxication whereas others, eg, stress-activated kinases, returned to baseline levels. Another mechanism that can be responsible for the observed dissociation of phospho-epitopes is that the phosphorylation sites in MBs have different half-lives of the bound phosphate. It is known that protein phosphatases are important regulators of steady-state cytokeratin phosphorylation.[20,40,60,64] Furthermore, different turnover rates were identified for the various phosphorylation sites on CK8 and CK18.[48] In contrast to CK8, which showed a higher steady-state phosphorylation in a variety of situations, including chronic intoxication of mice with GF or stimulation of PKC in cultured hepatocytes, CK18 had a lower steady state phosphorylation level because of rapid dephosphorylation by protein phosphatases.[17,19,64]

In summary, the applied phospho-cytokeratin antibodies proved to be a powerful tool, which allowed for the first time investigation of cytokeratin phosphorylation in human AH. The identification of the diverse phosphorylated serines on CK8 and CK18 in different phases of MB formation will help to elucidate the signals responsible for the activation of the corresponding protein kinases in future studies. The characterization of the signal transduction pathways will not only provide new insights into the pathogenesis of alcoholic liver disease, but also identify potential targets for new therapeutic approaches.

## *Acknowledgments*

We gratefully acknowledge the collaboration of Dr. R. Stauber and Dr. M. Trauner from the Department of Medicine as well as Dr. H.J. Mischinger and Dr. H. Hauser from the Department of Surgery, University of Graz, and thank them for providing us with liver tissue and patient data.

## References


1. Steinert PM, Roop DR: Molecular and cellular biology of intermediate filaments. Annu Rev Biochem 1988, 57:593–625
2. Fuchs E, Weber K: Intermediate filaments: structure, dynamics, function, and disease. Annu Rev Biochem 1994, 63:345–382
3. Julien JP: Neurofilaments and motor neuron disease. Trends Cell Biol 1997, 7:243–249
4. Jellinger K: New developments in the pathology of Parkinson's disease. Adv Neurol 1990, 53:1–16
5. Pollanen MS, Dickson DW, Bergeron C: Pathology and biology of the Lewy body. J Neuropathol Exp Neurol 1993, 52:183–191
6. Trojanowski JQ, Schmidt ML, Shin RW, Bramblett GT, Rao D, Lee VM: Altered tau and neurofilament proteins in neurodegenerative diseases: Diagnostic implications for Alzheimer's disease and Lewy body dementia. Brain Pathol 1993, 3:45–54
7. Goebel HH: Desmin-related myopathies. Curr Opin Neurol 1997, 10:426–429
8. Mallory FB: Cirrhosis of the liver: five different lesions from which it may arise. Bull Johns Hopkins Hosp 1911, 22:69–75
9. Denk H, Franke WW, Kerjaschki D, Eckersdorfer R: Mallory bodies in experimental animals and man. Int Rev Exp Pathol 1979, 20:77–121
10. Jensen K, Gluud C: The Mallory body: morphology, clinical and experimental studies (part 1 of a literature survey). Hepatology 1994, 20:1061–1077
11. Jensen K, Gluud C: The Mallory body: theories on development and pathological significance (part 2 of a literature survey). Hepatology 1994, 20:1330–1342
12. Lee MK, Cleveland DW: Neuronal intermediate filaments. Annu Rev Neurosci 1996, 19:187–217
13. Forno LS, Sternberger LA, Sternberger NH, Strefling AM, Swanson K, Eng L: Reaction of Lewy bodies with antibodies to phosphorylated and non-phosphorylated neurofilaments. Neurosci Lett 1986, 64: 253–258
14. Munoz DG, Greene C, Perl DP, Selkoe DJ: Accumulation of phosphorylated neurofilaments in anterior horn motorneurons of amyotrophic lateral sclerosis. J Neuropathol Exp Neurol 1988, 47:9–18
15. Trojanowski JQ, Lee VM: Phosphorylation of neuronal cytoskeletal proteins in Alzheimer's disease and Lewy body dementia. Ann NY Acad Sci 1994, 747:92–109
16. Goebel HH, Bornemann A: Desmin pathology in neuromuscular diseases. Virchows Arch B 1993, 64:127–135
17. Salmhofer H, Rainer I, Zatloukal K, Denk H: Posttranslational events involved in griseofulvin-induced cytokeratin cytoskeleton alterations. Hepatology 1994, 20:731–740
18. Kawahara H, Cadrin M, French SW: Ethanol-induced phosphorylation of cytokeratin in cultured hepatocytes. Life Sci 1990, 47:859–863
19. Cadrin M, McFarlane Anderson N, Aasheim LH, Kawahara H, Franks DJ, French SW: Modifications in cytokeratin and actin in cultured liver cells derived from griseofulvin-fed mice. Lab Invest 1995, 72:453–460
20. Yuan QX, Nago Y, Gaal K, Hu B, French SW: Mechanisms of Mallory body formation induced by okadaic acid in drug-primed mice. Exp Mol Pathol 1998, 65:87–103
21. Ku NO, Michie SA, Oshima RG, Omary MB: Chronic hepatitis, hepatocyte fragility, and increased soluble phosphoglycokeratins in transgenic mice expressing a cytokeratin 18 conserved arginine mutant. J Cell Biol 1995, 131:1303–1314
22. Diehl AM, Goodman Z, Ishak KG: Alcohol-like liver disease in nonalcoholics: a clinical and histologic comparison with alcohol-induced liver injury. Gastroenterology 1988, 95:1056–1062
23. French SW, Nash J, Shitabata P, Kachi K, Hara C, Chedid A, Mendenhall CL, VA Cooperative Study Group 119: Pathology of alcoholic liver disease. Sem Liver Dis 1993, 13:154–169
24. Hall P: Pathological spectrum of alcoholic liver disease. Alcoholic Liver Disease Pathology and Pathogenesis, 2nd ed. Edited by P Hall. London, Boston, Melbourne, Auckland, Edward Arnold, pp 41–68
25. Worman HJ: Cellular intermediate filament networks and their derangement in alcoholic hepatitis. Alcohol Clin Exp Res 1990, 14: 789–804
26. Zatloukal K, Kenner L, Preisegger KH, Denk H: Alcoholic liver disease: molecular-pathologic aspects. Verh Dtsch Ges Pathol 1995, 79:28–35
27. Denk H, Gschnait F, Wolff K: Hepatocellular hyalin (Mallory bodies) in long term griseofulvin-treated mice: a new experimental model for the study of hyalin formation. Lab Invest 1975, 32:773–776
28. Tsunoo C, Harwood TR, Arak S, Yokoo H: Cytoskeletal alterations leading to Mallory body formation in livers of mice fed 3,5-diethoxycarbonyl-1,4-dihydrocollidine. J Hepatol 1987, 5:85–97
29. Franke WW, Denk H, Schmid E, Osborn M, Weber K: Ultrastructural, biochemical, and immunologic characterization of Mallory bodies in livers of griseofulvin-treated mice: fimbrated rods of filaments containing precytokeratin-like polypeptides. Lab Invest 1979, 40: 207–220
30. Zatloukal K, Spurej G, Rainer I, Lackinger E, Denk H: Fate of Mallory body-containing hepatocytes: disappearance of Mallory bodies and restoration of the hepatocytic intermediate filament cytoskeleton after drug withdrawal in the griseofulvin-treated mouse. Hepatology 1990, 11:652–661
31. Preisegger KH, Zatloukal K, Spurej G, Denk H: Changes of cytokeratin filament organization in human and murine Mallory body-containing livers as revealed by a panel of monoclonal antibodies. Liver 1991, 11:300–309
32. Moll R, Franke WW, Schiller D, Geiger B, Krepler R: The catalog of human cytokeratins: patterns of expression in normal epithelia, tumors and cultured cells. Cell 1982, 31:11–24
33. Fuchs E, Coppock S, Green H, Cleveland D: Two distinct classes of epidermal keratin genes and their evolutionary significance. Cell 1981, 27:75–84
34. Franke WW, Denk H, Kalt R, Schmid E: Biochemical and immunological identification of cytokeratin proteins present in hepatocytes of mammalian liver tissue. Exp Cell Res 1981, 131:299–318
35. Denk H, Krepler R, Lackinger E, Artlieb U, Franke WW: Biochemical and immunological analysis of the intermediate filament cytoskeleton in human hepatocellular carcinomas and in hepatic neoplastic nodules of mice. Liver 1982, 2:165–175
36. Van Eyken P, Desmet VJ: Cytokeratins and the liver. Liver 1993, 13:113–122
37. Celis JE, Larsen PM, Fey SJ, Celis A: Phosphorylation of cytokeratin and vimentin polypeptides in normal and transformed mitotic human epithelial amnion cells: behavior of cytokeratin and vimentin filaments during mitosis. J Cell Biol 1983, 97:1429–1434
38. Zatloukal K, Denk H, Lackinger E, Rainer I: Hepatocellular cytokeratins as substrates of transglutaminase. Lab Invest 1989, 61:603–608
39. Chou CF, Omary MB: Phorbol acetate enhances the phosphorylation of cytokeratins 8 and 18 in human colonic epithelial cells. FEBS Lett 1991, 282:200–204
40. Omary MB, Baxter GT, Chou CF, Roipel CL, Lin WY, Strulovici B: PKC$\epsilon$-related kinase associates with, and phosphorylates cytokeratin 8 and 18. J Cell Biol 1992, 117:583–593
41. Omary MB, Ku NO, Liao J, Price D: Keratin modifications and solubility properties in epithelial cells and in vitro. Subcell Biochem 1998, 31:105–140
42. Ku NO, Liao J, Chou CF, Omary MB: Implications of intermediate filament protein phosphorylation. Cancer Metastasis Rev 1996, 15: 429–444
43. Chou CF, Omary MB: Mitotic arrest-associated enhancement of O-linked glycosylation and phosphorylation of human keratins 8 and 18. J Biol Chem 1993, 268:4465–4472
44. Liao J, Lowthert LA, Omary MB: Heat stress or rotavirus infection of human epithelial cells generates a distinct hyperphosphorylated form of keratin 8. Exp Cell Res 1995, 219:348–357
45. Baribault H, Blouin R, Bourgon L, Marceau N: Epidermal growth factor-induced selective phosphorylation of cultured rat hepatocyte 55-kD cytokeratin before filament reorganization and DNA synthesis. J Cell Biol 1989, 109:1665–1676
46. Liao J, Ku NO, Omary MB: Stress, apoptosis, and mitosis induce phosphorylation of human keratin 8 at ser-73 in tissues, and cultured cells: J Biol Chem 1997, 272:17565–17573
47. Ku NO, Omary MB: Identification of the major physiologic phosphorylation site of human cytokeratin 18: potential kinases and a role in filament reorganization. J Cell Biol 1994, 127:161–171
48. Liao J, Lowthert LA, Ku NO, Fernandez R, Omary MB: Dynamics of human cytokeratin 18 phosphorylation: polarized distribution of phosphorylated cytokeratins in simple epithelial tissues. J Cell Biol 1995, 131:1291–1301
49. Ku NO, Omary MB: Phosphorylation of human keratin 8 in vivo at

conserved head domain serine 23 and at epidermal growth factor-stimulated tail domain serine 431. J Biol Chem 1997, 272:7556–7564
50. Ku NO, Liao J, Omary MB: Phosphorylation of human keratin 18 serine 33 regulates binding to 14–3-3 proteins. EMBO J 1998, 17: 1892–1906
51. Zatloukal K, Denk H, Spurej G, Lackinger E, Preisegger KH, Franke WW: High molecular weight component of Mallory bodies detected by a monoclonal antibody. Lab Invest 1990, 62:472–434
52. Hutter H, Zatloukal K, Winter G, Stumptner C, Denk H: Disturbance of cytokeratin homeostasis in griseofulvin-intoxicated mouse liver. Lab Invest 1993, 69:576–582
53. Laemmli UK: Cleavage of structural proteins during the assembly of the head of bacteriophage T4. Nature 1979, 227:680–685
54. Towbin H, Staehelin T, Gordon J: Electrophoretic transfer of proteins from polyacrylamide gels to nitrocellulose sheets: procedures and some applications. Proc Natl Acad Sci USA 1979, 76:4350–4354
55. Lane B: Keratin diseases. Curr Opin Genet Dev 1994, 4:412–418
56. Fuchs E: The cytoskeleton and disease: genetic disorders of intermediate filaments. Annu Rev Genet 1996, 30:197–231
57. Ku NO, Wright TL, Terrault NA, Gish R, Omary MB: Mutation of human keratin 18 in association with cryptogenic cirrhosis. J Clin Invest 1997, 99:19–23
58. Toivola DM, Omary MB, Ku NO, Peltola O, Baribault H, Eriksson JE: Protein phosphatase inhibition in normal and keratin 8/18 assembly-incompetent mouse strains supports a functional role of keratin intermediate filaments in preserving hepatocyte integrity. Hepatology 1998, 28:116–128
59. Ku NO, Michie SA, Soetikno RM, Resurreccion EZ, Broome RL, Omary MB: Mutation of a major keratin phosphorylation site predisposes to hepatotoxic injury in transgenic mice. J Cell Biol 1998, 143:2023–2032
60. Omary MB, Ku NO: Intermediate filament proteins of the liver: emerging disease association and functions. Hepatology 1997, 25:1043–1048
61. Hoek JB, Thomas AP, Rooney TA, Higashi K, Rubin E: Ethanol and signal transduction in the liver. FASEB J 1992, 6:2386–2396
62. Chen J, Ishac EJN, Dent P, Kunos G, Gao B: Effects of ethanol on mitogen-activated protein kinase and stress-activated protein kinase cascades in normal and regenerating liver. Biochem J 1998, 334: 669–676
63. Yuan QX, Marceau N, French BA, Fu P, French SW: Mallory body induction in drug-primed mouse liver. Hepatology 1996, 24:603–612
64. Toivola DM, Goldman RD, Garrod DR, Eriksson JE: Protein phosphatases maintain the organization and structural interactions of hepatic keratin intermediate filaments. J Cell Sci 1997, 110:23–33